ELSEVIER

International Journal of Mass Spectrometry 210/211 (2001) 133–146

www.elsevier.com/locate/ijms

Proton affinity of deuterated acetonitrile estimated by the kinetic method with full entropy analysis‡

Taufika Islam Williams, Jeff W. Denault, R. Graham Cooks*

Department of Chemistry, Purdue University, West Lafayette, IN 47907-1393, USA

Received 26 December 2000; accepted 16 April 2001

Abstract

Branching ratios for the dissociation of proton-bound dimers of selected alkyl nitriles, $[R_1CN\cdots H+\cdots NCR_2]$, have been measured as a function of collision energy, using a triple quadrupole mass spectrometer. The system shows a small collision energy dependence consistent with small differences in entropy requirements for the competing fragmentation channels. The extended form of the kinetic method provides a value for the proton affinity and an approximate value for the relative entropy difference between the two dissociation channels (which corresponds approximately to the relative entropy of protonation of the two bases). A comparison is made between these results and those from earlier standard kinetic method data treatments. The proton affinity of d_3-acetonitrile, estimated by the extended kinetic method, is 186.3 ± 1.2 (±1.4) kcal mol^{-1}, where the standard deviation is given, followed by the 90% confidence limits in parentheses. The proton affinity of acetonitrile, estimated using the extended kinetic method as 188.2 ± 1.2 (±1.4) kcal mol^{-1}, is statistically the same as that obtained for d_3-acetonitrile. The relative entropies of protonation, $\Delta(\Delta S)$, for d_3-acetonitrile and acetonitrile, referenced to a series of alkyl nitriles, are 1.8 ± 0.3 (±0.3) and −1.1 ± 0.3 (±0.3) cal mol^{-1} K^{-1}, respectively. Direct comparison of the isotopomers of acetonitrile using the standard and extended kinetic methods was employed to arrive at a more accurate value for the proton affinity difference between d_3-acetonitrile and acetonitrile, and this method yielded a difference of ~0.2 kcal mol^{-1}. The direct comparison was also used to show that the proton affinity difference is a result of isotopic substitution. Normal secondary kinetic isotope effects were observed for the dissociation of the proton-bound dimer, $CH_3CN\cdots H^+\cdots CD_3CN$. The branching ratio, k_H/k_D, was constant at 1.2 over the laboratory collision energy range of 5–50 eV. (Int J Mass Spectrom 210/211 (2001) 133–146) © 2001 Elsevier Science B.V.

Keywords: Proton affinity; kinetic method; entropy analysis; kinetic isotope effect; nitriles

1. Introduction

The kinetic method for determining thermochemical properties is a relative method that is based on the rates of competitive dissociation of cluster ions containing the compound of interest and a suitable reference compound, bound through a central charged moiety [1–5]. This method has been used to measure a variety of thermochemical properties, including gas-phase acidities and basicities, proton affinities (PAs), ionization energies, polyatomic cation affinities, and electron affinities [4]. The kinetic method has also been applied to structural characterization, for

* Corresponding author. E-mail: cooks@purdue.edu

‡ Dedicated to Professor N.M.M. Nibbering on the occasion of his retirement and in recognition of his many contributions to gas-phase ion chemistry, his leadership in mass spectrometry, and his friendship.

PII S1387-3806(01)00455-9

example, recognition of agostic bonding in the gas phase [6] and, recently, chirality distinction and quantitation of enantiomers [7]. The standard form of the kinetic method [2–4] allows quantitative affinity determinations to be made provided certain limitations, such as the absence of reverse activation barriers and equal entropy changes for the two dissociation channels, are met [2–5].

In the specific case of PA determination, the fragmentation of a mass-selected proton-bound cluster ion, which dissociates competitively to yield the protonated monomers, is examined (Eq [1]).

$$A\cdots H^+\cdots B_i \xrightarrow{k_1} AH^+ + B_i \qquad A\cdots H^+\cdots B_i \xrightarrow{k_2} A + B_iH^+ \qquad (1)$$

The mass-selected dimeric ion is activated by collisions with a suitable gas, for example, argon, and the fragments that arise from collision-induced dissociation (CID) are mass analyzed. The determination of PA differences between the two monomers is made using Eq, (2), taking the ratio of the rate constants for the competitive dissociation channels of the dimer, k_1/k_2, as the ratio of the relative abundances of the individual protonated monomers, $[AH^+]/[BH^+]$:

$$\ln\frac{k_1}{k_2} = \ln\frac{[AH^+]}{[B_1H^+]} = \frac{PA(A) - PA(B)_i}{RT_{eff}}. \qquad (2)$$

In the standard kinetic method, a plot of $\ln(k_1/k_2)$ is made against $PA(B_1)$; namely, the known PA values of a series of reference compounds, B_i. The slope of the plot provides a value for the effective temperature (T_{eff}, discussed in more detail later), and the *x*-intercept gives a value for PA(A). The kinetic method has also been described using RRK and RRKM theories in which the branching ratio can be related to the dissociation energetics without invoking an equilibrium temperature [8,9].

A more complete treatment of the kinetic method has been developed that allows deconvolution of the enthalpic and entropic contributions for systems that have a nonzero difference between the entropy changes associated with each dissociation channel [10–12]. This extended kinetic method allows more accurate enthalpic values to be obtained. By acquiring abundance ratio data at several collision energies and, therefore, at several effective temperatures, it is possible to determine $\Delta(\Delta H)$ and $\Delta(\Delta S)$, where the Δ refers to the two channels shown in Eq. (1). That is, the enthalpy and entropy changes for each of the dissociation channels of the proton-bound cluster ion refer to changes between the protonated monomer; that is, the products on one hand and the reactant cluster ion on the other. The differences between the two dissociation channels are, to a good approximation, the differences in reaction enthalpies and entropies of the protonation reactions: ($B + H^+ \rightarrow BH^+$, $B_i + H^+ \rightarrow B_iH^+$) for the constituent monomers; that is, $\Delta(\Delta H) = \Delta H_{rxn}(A) - \Delta H_{rxn}(B_i)$ and $\Delta(\Delta S) = \Delta S_{rxn}(A) - \Delta S_{rxn}(B_i)$. The term $\Delta(\Delta H)$ is the difference in proton affinities of the two ligands, while $\Delta(\Delta S)$ is the difference in the protonation entropy of the two ligands.

From unimolecular rate theory [1–3], the ratio of the rate constants for Eq. (1) can be expressed as

$$\ln(k_1/k_2) = \ln[AH^+]/[B_iH^+] = 1n\,(Q_1^{\ddagger}/Q_2^{\ddagger}) + [\epsilon_0(2) - \epsilon_0(1)]/RT_{eff}, \qquad (3)$$

where $[AH^+]$ and $[B_iH^+]$ correspond to the abundances of the protonated analyte and the protonated reference compound; $Q_1^{\ddagger}$ and $Q_2^{\ddagger}$ are the partition functions of the activated complex for the formation of ($AH^+ + B_i$), and ($A + B_iH^+$), respectively; $\epsilon_0(1)$ and $\epsilon_0(2)$ are the respective critical energies for dissociation; T_{eff} is the effective temperature of the dimer ion undergoing dissociation, taken as equal for the two channels. The activated complexes corresponding to each of the two competitive dissociation channels are in equilibrium with the corresponding activated molecules and, hence, with each other. The effective temperature, T_{eff} determined from the kinetic method plots is an average value for the two dissociation channels and represents the degree of internal excitation of the proton-bound dimer under-

going dissociation. The meaning of effective temperature has recently been discussed in detail and equated to the internal energy of the activated complex or, similarly, to the temperature of those ions that have sufficient internal energy to dissociated [14–16]. The internal energy of the activated cluster ion may be varied by changing either the collision energy or the collision gas pressure, and T_{eff} changes accordingly. With the assumption of zero or equal reverse-activation barriers, the difference in critical energies for the competitive dissociation channels is equal to the difference in PAs, so one can write

$$\ln(k_1/k_2) = \ln(Q_1^{\ddagger}/Q_2^{\ddagger}) + \text{PA(A)}/(RT_{\text{eff}}) - \text{PA}(B_i)/(RT_{\text{eff}}). \quad (4)$$

Furthermore, with the assumptions already noted, the partition function term, $\ln(Q_1^{\ddagger}/Q_2^{\ddagger})$, can be replaced by $-\Delta(\Delta S)/R$, the difference in the average value of the protonation entropies of A and that of B_i. Hence,

$$\ln(k_1/k_2) = -\Delta(\Delta S)/R + \text{PA}(A)/(RT_{\text{eff}}) - \text{PA}(B_i)/(RT_{\text{eff}}). \quad (5)$$

For a series of reference bases that are structurally dissimilar from the analyte but are similar in structure among themselves, the entropy term $-\Delta(\Delta S)/R$ in Eq. (5) may be nonzero but still constant. The plot of $\ln(k_1/k_2)$ versus $\text{PA}(\text{B}_i)$ will then still produce a linear correlation. Therefore, when the difference in entropy changes between the two dissociation channels is kept constant, that is, when the reference compounds B_i are chemically similar among themselves, the extended kinetic method [10–12] can be applied using Eqs. (6) and (7), as defined:

$$\ln(k_1/k_2) = [\text{PA(A)}/(RT_{\text{eff}}) - \Delta(\Delta S)/R] - \text{PA}(B_i)/(RT_{\text{eff}}); \quad (6)$$

$$\text{GB}^{\text{app}}(A)/RT_{\text{eff}} = \text{PA}(A)/(RT_{\text{eff}}) - \Delta(\Delta S)/R. \quad (7)$$

The slope and intercept of the linear regression of the plot $\ln\{[AH^+]/[B_iH^+]\}$ versus $\text{PA}(B_i)$, the known PA values of the reference compounds B_1 (Eq. [6]), provide values for the effective temperature, T_{eff} and $\text{GB}^{\text{app}}(\text{A})$, respectively. The GB^{app} value determined for a given T_{eff} value differs from the true gas-phase basicity of the analyte by the inclusion of the term containing $\Delta\text{S}(\text{B}_i)$, the protonation entropy of the reference compound, assumed to be temperature independent, a point discussed in greater length elsewhere [17]

$$\text{GB}^{\text{app}}(A) = \text{PA}(A) - T_{\text{eff}}\Delta(\Delta S). \quad (8)$$

The contributions of enthalpy and entropy to GB^{app} can be determined through a second plot requiring the measurement of product ion abundance ratios at different values of T_{eff}, which can be achieved by varying the collision energy in the CID experiment. The second plot, constructed from the negative of the slopes and the intercepts of multiple collision energy experiments (plots of $\text{GB}^{\text{app}}[A^+]/RT_{\text{eff}}$ versus $1/RT_{\text{eff}}$ at several values of T_{eff}), allows the enthalpic and entropic quantities to be determined. The PA of the analyte, A, is obtained from the slope of the second plot, whereas $\Delta(\Delta S)$, the entropy of protonation for A relative to the average value for the set of compounds B_i, is estimated from the y-intercept [4]. Plotted in this fashion, the second plot has a high correlation coefficient, which has been attributed to consistency in the entropic component, but the correlation is imposed by the plotting method.

To remove the covariance of the slope and the intercept, a more rigorous treatment has been proposed by Armentrout [1]. Appropriate statistical procedures remove the covariance of the slope and intercept of the first plot and provide a simple means of analyzing the uncertainties in the thermodynamic quantities obtained [1] The practical difference between the two methods does not lie in the quantitative results themselves but, rather, in the errors associated with the values.

Kinetic isotope effects (KIEs), changes in the reaction rates brought about by isotopic substitution, were also measured in this study. KIEs provide important information on ion and neutral structures as well as on reaction mechanisms [18]. Primary kinetic isotope effects are those in which the bond to the

isotopic atom is broken in the rate-determining step, whereas in secondary kinetic isotope effects (SKIE) the bond to the isotopic atom(s) remains intact throughout the reaction. In many cases, reaction rates are affected by a combination of primary and secondary isotope effects [18]. As mentioned above, the standard kinetic method provides convenient access to ion affinities when the vibrational frequencies of the two ion–molecule bonds in the dimer are very similar. The standard kinetic method, therefore, is particularly suitable for measuring ion affinity differences between isotopomers. The relative difference in affinity or bond dissociation energy, $\Delta(\Delta H)$, obtained in this manner should allow accurate measurement of kinetic isotope effects [19].

In previous ion trap experiments from this laboratory, the kinetic method was used to detect very small proton affinity differences arising from deuterium substitution in 2-pentanone and acetophenone [20]. A normal secondary kinetic isotope effect was observed for $CH_3COCD_2CH_2CH_3$, that is, the nondeuterium-labeled ketone was determined to have the higher PA. For $PhCOCD_3$, an inverse secondary isotope effect was observed. However, interpretation of the behavior of both systems is complicated by the possibility of keto-enol tautomerism in the ions, in the clusters, and in the corresponding neutral molecules.

Bierbaum and co-workers [21] employed a tandem flowing afterglow-selected ion flow tube (FA-SIFT) to measure the gas-phase acidities of deuterated ethanols using the kinetic method. Both α- and β-deuterated ethanols were determined to be weaker acids than the undeuterated ethanol, with α-deuteration having the more pronounced effect. The acidities relative to ethanol, $\Delta H_{acid,298K}(CH_3CH_2OH) = 377.5 \pm 2$ kcal mol^{-1}, were determined to be $\Delta\Delta H_{acid}(CD_3CH_2OH) = 0.20 \pm 0.15$ kcal mol^{1}, $\Delta\Delta H_{acid}(CH_3CD_2OH) = 0.35 \pm 0.15$ kcal mol^{-1}, and $\Delta\Delta H_{acid}(CD_3CD_2OH) = 0.50 \pm 0.15$ kcal mol^{-1}. The authors suggested that the change in acidity of the deuterated species is indicative of the zero-point energy (ZPE) differences between deuterated and undeuterated alkoxides being smaller than the corresponding differences in the alcohols.

In a related study, O'Hair and coworkers [22] utilized the kinetic method to investigate the effects of isotopic substitution on the gas-phase PA of glycine. Their study was the first to investigate the effects of isotopic substitution on the gas-phase proton affinity of this amino acid. The order of proton affinities of two isotopomers of glycine relative to the unlabeled amino acid was determined to be $PA(H_2NCD_2CO_2H) = 886.05 \pm 0.63$ kJ mol$^{1} \geq PA(H_2{}^{15}NCH_2CO_2H) = 885.75 \pm 0.42$ kJ mol$^{-1} \geq PA(H_2NCH_2CO_2H) = 885.3$ kJ mol^{1}. Within the limits of experimental error, the proton affinities of glycine and its ^{15}N isotopomer were identical, while a small but significant difference existed between the proton affinities of the d_2-isotopomer relative to glycine.

Gozzo and Eberlin [19] employed a pentaquadrupole mass spectrometer to study the kinetic isotope effects associated with protonation versus deuteration, also by using the kinetic method. The sensitivity of the kinetic method to small variations in proton affinity and the suitability of tandem-in-space pentaquadrupole mass spectrometry allowed them to measure quite accurately the primary as well as secondary KIEs on PAs. These authors estimated acetonitrile to have a higher PA than deuterated acetonitrile from the dissociation of the proton-bound dimer, $CH_3CN\cdots H^+\cdots CD_3CN$, that is, a normal secondary kinetic isotope effect, was observed ($k_H/k_D = 1.32$) [19]. These experiments were performed at a single collision energy (15 eV) using argon as the target gas.

In this study, we employ the kinetic method to determine the PA of deuterated acetonitrile (CD_3CN) by applying the statistical treatment set out by Armentrout [1]. We also investigate the effects of deuterium substitution on the properties of selected proton-bound nitrile dimers, using propionitrile, butyronitrile, and valeronitrile as reference bases. The proton affinities and associated relative entropies of protonation for acetonitrile and d_3 acetonitrile are determined and compared. Comparisons are made between the results of the Fenselau and Wesdemiotis method and the Armentrout treatment. To extend the work of Gozzo and Eberlin, a range of collision energies (5–50 eV) is used to determine whether entropic effects substantially influence the dissociation of the

proton-bound dimers of deuterated and nondeuterated acetonitrile.

2. Experimental

Mass spectrometric experiments were performed using a Finnigan TSQ 700 triple quadrupole mass spectrometer (Finnigan MAT, San José, CA). All compounds were commercially available (Aldrich Chemical, Milwaukee, WI) and used as received. Pairs of nitriles (acetonitrile or deuterated acetonitrile, paired with a reference compound or with each other) were combined in a 1:1 ratio and introduced into the ion source through a Granville Phillips variable leak valve (Granville Phillips, Boulder, CO) at sufficient pressures to create chemical ionization conditions in the source (estimated pressure 0.5 Torr). For all experiments, the source temperature was maintained at 100 °C and the manifold at 70 °C.

Ions corresponding to the mass-to-charge ratio of the proton-bound dimers were mass selected using the first quadrupole. Collisional activation of the dimer was achieved in the second quadrupole at laboratory collision energies ranging from nominal 5 to 50 eV, using an argon target at pressures corresponding to single collision conditions (i.e., primary ion beam attenuated by $<$20%) [23]. The product ion mass spectra were recorded by scanning the third quadrupole. Peak ratio measurements were made in triplicate and had relative standard deviations of $\approx$5%. Mass-to-charge ratios are reported using the Thomson unit (1 Th = 1 atomic mass per unit positive charge) [24].

3. Results and Discussion

3.1. Cluster ion structure

The structures of cluster ions composed of a charged moiety and two nitriles has been of interest to our research group. Recently, it was shown that cluster ions composed of two nitriles (e.g.), acetonitrile and butyronitrile) and the methyl cation can result from initial N-methylation of one of the nitriles followed by the formation of a covalent C–N bond between the methylated nitrile and the neutral nitrile [25]. The two isomeric structures of the dimeric cluster ion are separated by a large barrier and are unable to interconvert before dissociation. While a covalently bound structure might be involved in the case of the protonated dimers of alkyl nitriles, it is likely that the two isomeric structures are not separated by a large barrier and, as such, are able to equilibrate before dissociation. Evidence for this is found in the fact that the fragmentation behavior is independent of partial pressure of the monomers and that the kinetic method gives thermochemical data that agree with literature values for acetonitrile. Neither of these situations were obtained in the case of the methylated dimers.

The results obtained for the dissociation of the protonated dimer of acetonitrile and d_3-acetonitrile, compounds whose proton affinities are not significantly different [19], suggest that the cluster ion is in a shallow potential-energy well. For a range of collision energies (5–50 eV), the branching ratio remains relatively constant with only a very slight decrease with increasing collision energy. This result further suggests that the k(ϵ) versus ϵ plots for the dissociation of this cluster ion rise sharply at low energies and rapidly level off at higher collision energies. These results are consistent with the proton-bound dimer structure that we assume in the remainder of the study to be formed under the conditions used here.

The effects of isotopic substitution on the dissociation of amines have been examined by Norman and McMahon [26]. These authors observed different kinetic isotope effects for the dissociation of the proton-bound dimer of acetonitrile and d_3-acetonitrile depending on the ion source conditions for the formation of the cluster ion, namely; an inverse KIE was observed under low-pressure ionization and a normal KIE was observed under high-pressure ionization. These differences may be the result of the formation of covalent as well as proton-bound structures, as discussed above. The high-pressure ionization KIE observed by Norrman and McMahon is similar to that reported here.

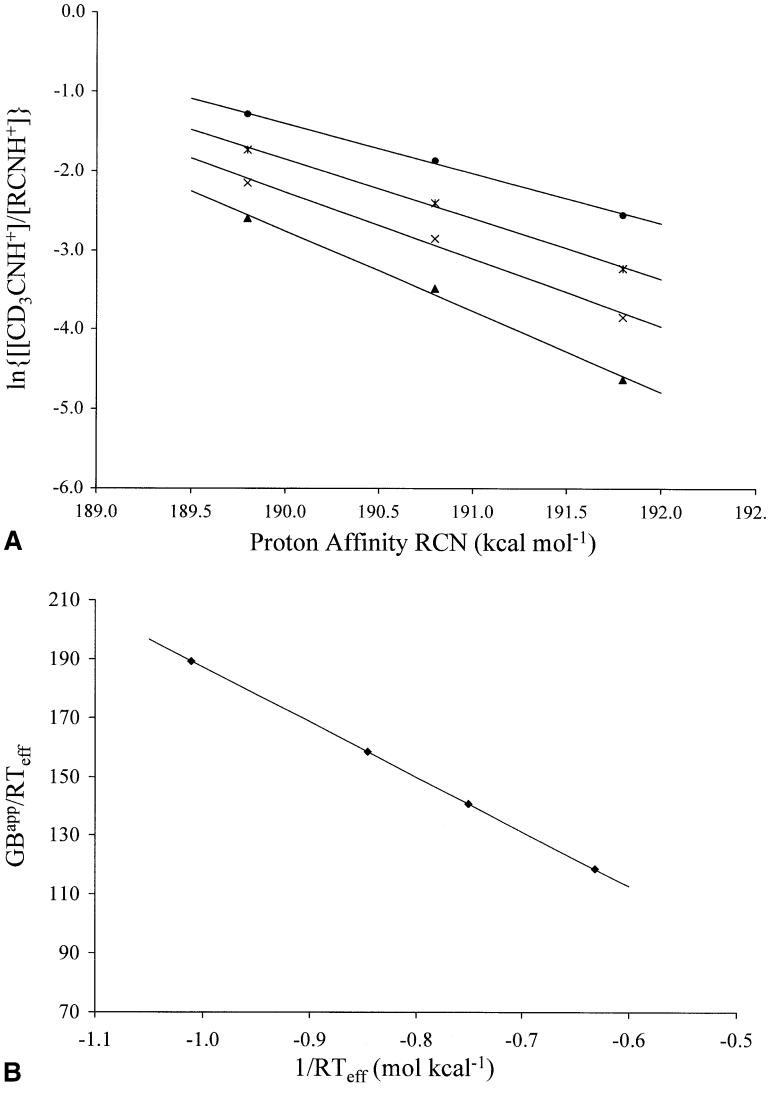

Fig. 1. (a) Standard kinetic method plot for the determination of the proton affinity (PA) of CD_3CN; plot of $\ln[RCNH^+]/[CD_3CNH^+]$ versus $PA(RCNH^+)$ (kcal mol^{-1}) for $R = C_2H_5$, C_3H_7 and C_4H_9. Four collision energies—5 (▲), 10 (×), 20 (*), and 50(●) eV—were used in the experiments. (b) Double plot method of Fenselau/Wesdemiotis for the determination of the proton affinity of CD_3CN; plot of GB^{app}/RT_{eff} versus l/RT_{eff}. The slope obtained from the plot $= -PA\ (CD_3CN) = -186.3 \pm 0.2\ (\pm 0.2)$ kcal mol^{-1} so, PA $(CD_3CN) = 186.3 \pm 0.2\ (\pm 0.2)$ kcal mol^{-1}. The intercept $= -\Delta(\Delta S)/R = -0.9 \pm 0.1\ (\pm 0.1)$, so $\Delta(\Delta S) = 1.8 \pm 0.3\ (\pm 0.3)$ cal mol^{-1} K^{-1}. Correlation coefficient $(R^2) = 1.00$.

3.2. Determination of the proton affinity of CD_3CN and CH_3CN

Experiments were performed using CD_3CN, a compound having unknown PA, to compare the Fenselau/Wesdemiotis and Armentrout methods of data analysis for the determination of PAs and relative entropies of protonation. The determination of $PA(CD_3CN)$ was made using the standard kinetic method plot, $\ln(k_B/k_B)$ versus $PA(B_i)$ (Fig. 1a), where B_i is a set of reference compounds of known PA, including propionitrile, butyronitrile, and valeroni-

Table 1
Apparent values of the proton affinity of CD_3CN obtained from various collision energy experiments

Collision energy (eV)	Apparent proton affinity (CD_3CN) (kcal/mol)[a]
5	187.3 ± 21.8 (± 36.7)
10	187.3 ± 28.0 (± 47.2)
20	187.5 ± 17.4 (± 29.4)
50	187.8 ± 11.3 (± 19.1)

Note. The proton affinities were determined from the x-intercepts of the standard kinetic method plots.

[a]Values given as apparent proton affinity ± standard deviation (±90% confidence interval).

trile. The measured values for the PA of CD_3CN at different collision energies are given in Table 1. These values fall within the narrow range of 187.3–187.8 kcal mol^1, and the average of these numbers might be taken to yield a good estimate of the PA of CD_3CN. The values obtained from the standard kinetic method are slightly higher than expected on the basis of the literature PA of CH_3CN, 186.2 kcal mol^{-1} [27], and the relative magnitudes of the two values correspond to the normal kinetic isotope effect observed by Eberlin et al [19]. The higher value of the d_3-isotopomer are reasonably interpreted as the result of isotopic substitution, although one cannot exclude the possibility of errors in the PA determination by the standard kinetic method caused by entropy effects in the dissociation of the proton-bound cluster ions. Entropy effects can be corrected for by using the extended kinetic method, and this was, therefore, done.

The Fenselau/Wesdemiotis treatment of the kinetic method is based on Eq. (6), where the slope and the intercept of the plot $\ln(k_1/k_2)$ versus $PA(B_i)$ are equal to $-1/RT_{eff}$ and $PA(A)/(RT_{eff}) - \Delta(\Delta S)/R$, respectively. Plots based on this equation are shown in Fig. 1. There are two sets of plots: the first corresponds to the standard kinetic method, whereas the second, or double, plot in this analysis is constructed from the slopes and intercepts of the initial plot using experimental data taken at a number of collision energies. The slope of the linear correlation for the double plot for CD_3CN is equal to -PA(*A*), and the *y*-intercept is equal to $-\Delta(\Delta S)/R$. A simple and unweighted statistical analysis of these data leads to a value for $PA(CD_3CN)$ of 186.4 ± 0.2 (±0.2) kcal mol^{-1} and a value for $\Delta(\Delta S)$ of 1.7 ± 0.3 (± 0.4) cal mol^{-1} K^{-1}, where the standard deviation and the 90% confidence interval follow the value. However, simple analysis fails to weight accurately the uncertainties in both the *x* and *y* directions for the points of the second plot [1]. When the data are appropriately weighted (Fig. 1b), the proton affinity of CD_3CN is estimated to be 186.3 ± 0.2 (±0.2) kcal mol^1 and $\Delta(\Delta S)$ = 1.8 ± 0.3 (± 0.3) cal mol^1K^{-1}.

The most important feature of the second plot in the Fenselau/Wesdemiotis treatment is the fact that it is extraordinarily linear, demonstrated by a regression coefficient (r^2) of unity. Indeed, *every* case examined using this method has shown regression coefficients very close to unity ($r^2 \geq 0.999$). The slope and intercept used to describe the initial kinetic method plot, on which this method is based, are strongly correlated. This can be explicitly shown by the covariance between the slope and the *y*-intercept. Furthermore, in the expression for the intercept (Eq. [8]), PA(*A*) values are not dependent on temperature, and if $\Delta(\Delta S)$ is small, $GB^{app}(A)$ will show only a small dependence on temperature. Hence, the linearity of the second plot simply demonstrates that both the *x* parameter ($1/RT_{eff}$) and *y* parameter ($GB^{app}(A)/RT_{eff}$) are strongly dependent on the effective temperature. The correlation between these two quantities is excellent, even when the determination of T_{eff} is rather imprecise [1].

Armentrout [1] has applied a statistically rigorous analysis based on the same methodology. He outlined several approaches that lead to similar results, with one of the treatments rigorously eliminating the strong covariance between the slope and intercept and also being simple to apply. Because the slope and the intercept of the linear correlation of Eq. (6), shown in Fig. 1b, are strongly correlated, small changes in the slope result in relatively large changes in the *y*-intercept, attested to by the large uncertainties in the *y*-intercept. Through statistical analysis, Armentrout was able to show that this strong correlation was caused by the covariance between the slope and the

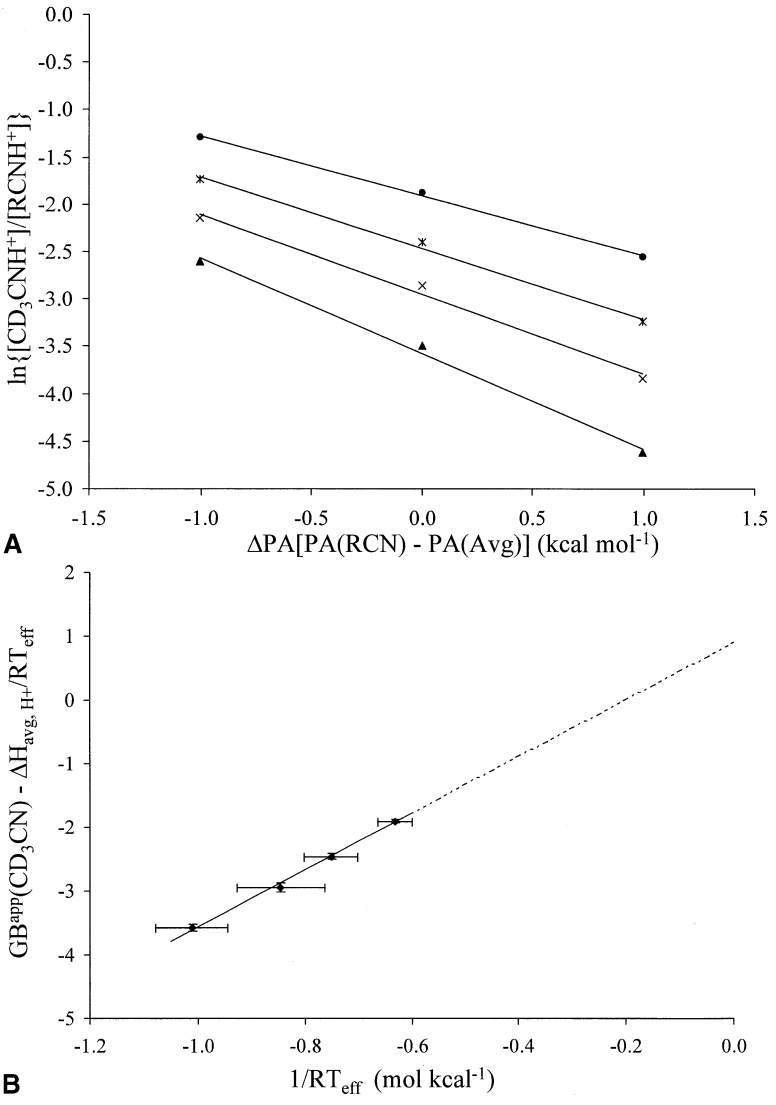

Fig. 2. (a) Armentrout method for the determination of the proton affinity (PA) of CD_3CN; plot of $\ln[RCNH^+]/[CD_3CNH^+]$ versus ΔPA [(PA(Ref) − PA(Avg)], where R = C_2H_5, C_3H_7, and C_4H_9. Four collision energies—5 (▲), 10 (×), 20 (*), and 50 (●) eV—were used in the experiments. (b) Double plotting method of Armentrout for the determination of the proton affinity of CD_3CN; plot of $[\Delta GB^{app}(CD_3CN) - \Delta H_{avg,H+}]/RT_{eff}$ versus $1/RT_{eff}$. The slope obtained from the plot = PA(CD_3CN) − PA(Avg) = 4.5 ± 0.2 (± 0.2) kcal mol^{-1}; so, PA (CD_3CN) = 186.3 ± 1.2 (± 1.4) kcal mol^{-1}. The intercept = $-\Delta(\Delta S)/R$ = −0.9 ± 0.1 (± 0.1), so $\Delta(\Delta S)$ = 1.8 ± 0.3 (± 0.3) cal mol^{-1} K^{-1}. Correlation coefficient (R^2) = 0.996.

y-intercept, as uncorrelated quantities would have a covariance of zero [1].

The correlation between the slope and intercept of a linear regression analysis was removed by plotting *y* (from Fig. 1a) versus $x_i' = x_i - x_{avg}$ The slope (m) of this graph is the same as that obtained by the Fenselau and Wesdemiotis data treatments, but in this case, the *y*-intercept (y_{01}') is an interpolated point. Such a plot is shown in Fig. 2a. Compared to extrapolation, the *y*-intercept determined by interpolation is much more accurate.

The slope of the initial kinetic method plot ob-

tained using the Armentrout analysis detailed above is equal to $-1/RT_{eff}$ and the *y*-intercept is given by

$$y'_{01} = [GB^{app}(A) - PA_{avg}]/RT_{eff}$$
$$= [PA(A) - PA_{avg}]/(RT_{eff}) - \Delta(\Delta S)\,R \qquad (9)$$

The effective temperatures for CD_3CN for the collision energies reported here are given in Table 2. Based on Eq. (9), a plot of the intercept versus the negative of the slope will yield a new correlation having a slope equal to $[PA(A) - PA_{avg}]$ and a *y*-intercept equal to $-\Delta(\Delta S)/R$. It can be seen that the intercept is the same as that found using the Fenselau and Wesdemiotis plotting method, but the slope is now related explicitly to PA_{avg} Fig. 2b illustrates the result of this plotting method. Employing an adequately weighted linear regression analysis, values obtained for the slope and *y*-intercept are 4.5 ± 0.2 (± 0.2) kcal mol^{-1} and −0.9 ± 0.1(± 0.1) kcal mol^{-1}, respectively. Given PA_{avg} = 190.8 kcal mol^{-1} for the reference compounds used, we estimate the $PA(CD_3CN)$ to be 186.3 ± 1.2 (± 1.4) kcal mol^{-1} and $\Delta(\Delta S)$ = 1.8 ± 0.3 (± 0.3) cal mol^{-1} K^{-1}. It is important to note that while the values obtained for the PA and $\Delta(\Delta S)$ are nearly the same as in the earlier treatment, the magnitude of the uncertainties obtained with the Armentrout method are larger than those obtained by the Fenselau/Wesdemiotis method. This is because error analysis in the Armentrout method is a much better representation of the actual errors associated with the experiment. The *unweighted* correlation coefficient of this plot (r^2) is 0.996, and it is not as linear as the plot of Fig. 1b. The correlation coefficients are calculated on the basis of the assumption that all data points carry equal weighting, regardless of the size of the errors associated with them. Fig. 2b is more representative of how well the assumptions pertaining to $\Delta(\Delta S)$ are followed [1]: It should be noted that the uncertainty in PA(*A*) includes the uncertainty in the literature PAs of the reference bases. Furthermore, in the expression for the intercept in the double plot (eq. [8]), the $GB^{app}(A)$ and PA(*A*) values do not vary strongly with temperature, and $\Delta(\Delta S)$ tends to be small, for the systems examined [1].

To investigate the effects of deuterium substitution, the proton affinity of acetonitrile was also determined using the same references and experimental conditions as used for d_3-acetonitrile. The standard kinetic method and the Armentrout treatment were employed in the determination of $PA(CH_3CN)$ and $\Delta(\Delta S)$. The effective temperatures obtained from the standard kinetic method plots are given in Table 2. The apparent PAs derived by the standard kinetic method for CH_3CN are given in Table 3. Note that the normal KIE observed with an apparent PA of CH_3CN is greater than the apparent PA of CD_3CN (Table 1) at lower collision energies, where entropic effects can be assumed to be negligible. The higher collision energy data will be discussed further below. The double plot described by Armentrout is given in Fig. 3. A properly weighted linear regression analysis of the second plot yields values for the slope and *y*-intercept, corresponding to $PA - PA_{avg}$ and $\Delta(\Delta S)$, respectively, of 2.6 ± 0.2 (± 0.2) kcal mol^{-1} and 0.6 ± 0.1 (±0.2) Given that for the reference compounds PA_{avg} = 190.8 kcal mol^{-1}, $PA(CH_3CN)$ was calculated to be

Table 2
Effective temperatures (T_{eff}) obtained from experiments at various collision energies

Collision energy (eV)	T_{eff}(K)[a]	T_{eff}(K)[b]
5	498 ± 33 (± 60)	416 ± 3 (± 6)
10	595 ± 58 (± 97)	568 ± 9 (± 16)
20	670 ± 44 (± 74)	718 ± 96 (± 161)
50	797 ± 39 (± 66)	967 ± 21 (± 35)

[a]Values obtained for the proton affinity determination of CD_3CN.
[b]Values obtained for the proton affinity determination of CH_3CN.

Table 3
Apparent values of the proton affinity of CH_3CN obtained from experiments at various collision energies

Collision energy (eV)	Apparent proton affinity (CH_3CN) (kcal/mol)[a]
5	187.8 ± 2.9 (± 4.9)
10	187.5 ± 4.9 (± 8.3)
20	187.3 ± 33.5 (± 56.4)
50	187.2 ± 4.1 (± 7.0)

Note. The proton affinities were determined from the x-intercepts of the standard kinetic method plots.
[a]Values given as apparent proton affinity ± standard deviation (± 90% confidence interval).

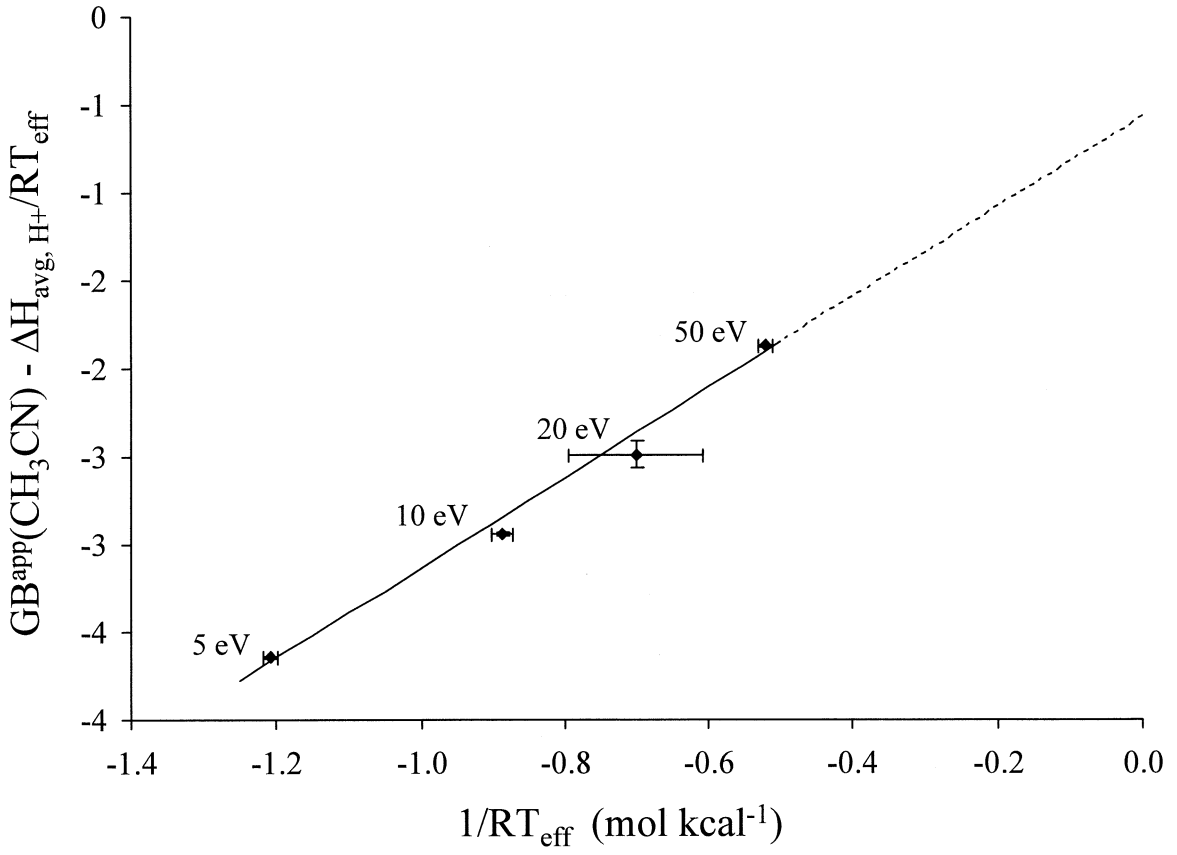

Fig. 3. Double plotting method of Armentrout for the determination of the proton affinity (PA) of CH_3CN; plot of $[\Delta GB^{app}(CH_3CN) - \Delta H_{avg,H+}]/RT_{eff}$ versus $1/RT_{eff}$. The slope obtained from the plot = $PA(CH_3CN) - PA(Avg) = 2.6 \pm 0.2$ (± 0.2) kcal mol^{-1}; so, $PA(CH_3CN) = 188.2 \pm 1.2$ (± 1.4) kcal mol^{-1}. The intercept = $-\Delta(\Delta S)/R = 0.6 \pm 0.1$ (± 0.2). So, $\Delta(\Delta S) = -1.1 \pm 0.3$ (± 0.3) cal mol^{-1} K. Correlation coefficient (R^2) = 0.989.

188.2 ± 1.2 (±1.4) kcal mol^{-1} and $\Delta(\Delta S)$ was determined as −1.1 ± 0.3 (±0.3) cal mol^{-1} K^{-1}. The quantitative values are very similar to those obtained (details not shown) using the Fenselau/Wesdemiotis method of data analysis, 188.2 ± 0.2 (±0.2) kcal mol^{-1} and −1.1 ± 0.3 (±0.3) cal mol^{-1} K^{-1} respectively. Once again, the errors obtained using the Armentrout method are larger. The *unweighted* correlation coefficient of this plot (r^2) is 0.989. The literature value for the PA of CH_3CN is 186.2 ± 2 kcal mol^{-1}, and the ranges for the literature (184.2–188.2 kcal mol^{-1}) and the experimental values (187.0–189.4 kcal mol^{-1}) of the PA of CH_3CN overlap.

The PA of CH_3CN (188.2 ± 1.2 [±1.4] kcal mol^{-1}) was determined, by the Armentrout method, to be higher than the PA of CD_3CN (186.3 ± 1.2 [±1.4] kcal mol^{1}). The 90% confidence levels for both $PA(CH_3CN)$ and $PA(CD_3CN)$ are 1.4 kcal mol^{-1}. So, the acceptable range for $PA(CH_3CN)$ at this confidence level is 186.9–189.6 kcal mol^{-1}, whereas the range for $PA(CD_3CN)$ is 185.0–187.7 kcal mol^{-1}. Because there is overlap between the two ranges, it can be concluded that the 1.9 kcal mol^{-1} difference in the proton affinities between CH_3CN and CD_3CN might be caused by statistical error and not necessarily by isotopic substitution. Furthermore, at the 90% confidence level, the range for the experimentally determined PA values of both CH_3CN and CD_3CN overlap with the literature value (186.2 kcal mol^{-1}).

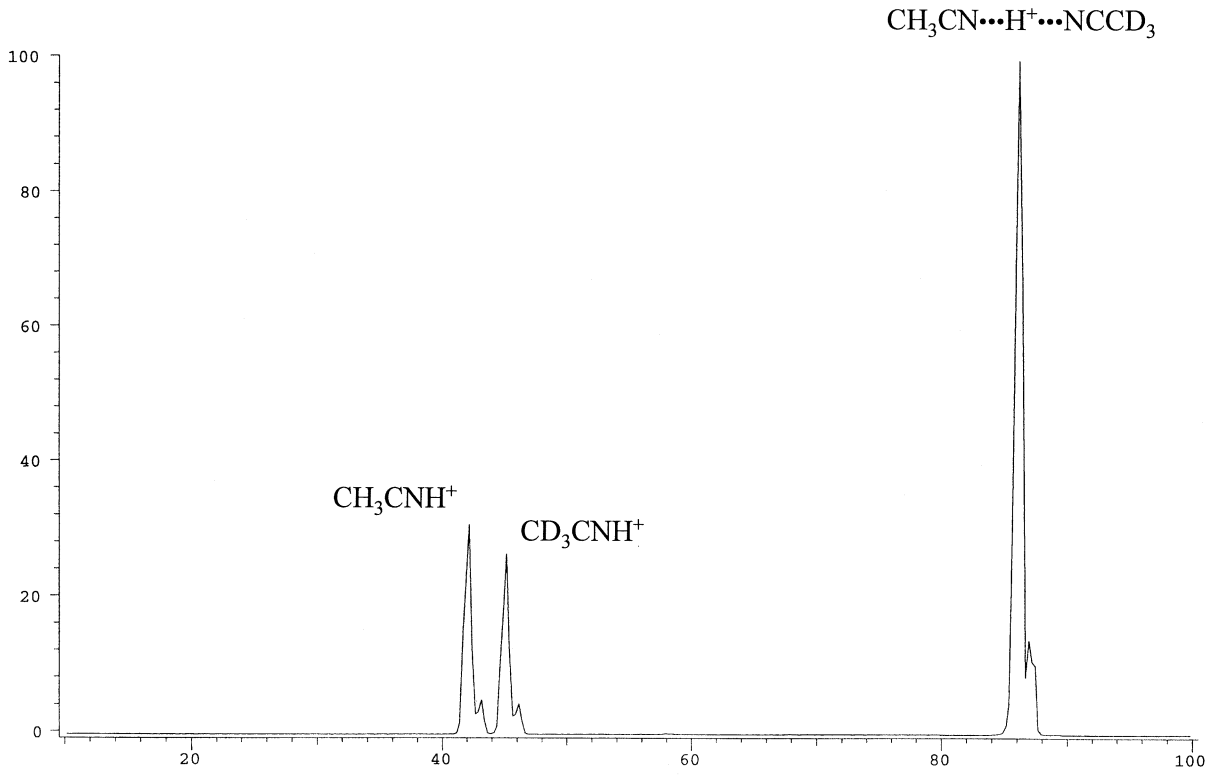

Fig. 4. CID mass spectrum of CH_3CN----H^+----CD_3CN with argon at 5 eV collision energy.

The relative entropies of protonation, $\Delta(\Delta S)$, for d_3-acetonitrile and acetonitrile, referenced to a series of alkyl nitriles, are 1.8 ± 0.3 (±0.3) cal mol^{-1} K^{-1} and −1.1 ± 0.3 (±0.3) cal mol^{-1} K^{-1}, respectively. The difference in these values (which are of opposite sign) suggests a real difference in the entropy of protonation of d_3-acetonitrile and acetonitrile.

3.3. Kinetic isotope effects on the dissociation of the cluster ion, CH_3CN H^+ $NCCD_3$

The 1.9 kcal mol^{-1} difference between the two PA values estimated by the kinetic method experiments is within statistical uncertainty and is larger than one would expect for isotopic substitution. Indeed, the experimental results of Eberlin et al. [19], suggest that the difference in PA between acetonitrile and d_3-acetonitrile is on the order of 0.3 kcal mol^{-1}. We investigated the PA difference further by performing similar experiments in which the two acetonitriles were compared directly. The dissociation of the proton-bound cluster ion composed of acetonitrile and d_3-acetonitrile, illustrated by the product ion MS/MS spectrum shown in Fig. 4, shows a greater abundance of the protonated acetonitrile compared with the abundance of the protonated d_3-acetonitrile. The branching ratio for this cluster ion is 1.2. This result is in agreement with the observations of Eberlin and Gozzo, where the ratio of rate constants for the two dissociating pathways, $k(CH_3CNH^+)/k(CD_3CNH^+)$, was estimated to be 1.32 [19]. The slight difference between the two results likely arises from the fact that the experiments were performed on different instruments and, hence, used different time scales, where the ions have different internal energies.

It is expected that as the collision energy is increased, the branching ratio will decrease and the effective temperature of the activated proton-bound

Table 4
Observed kinetic isotope effect (KIE) for the dissociation of $CH_3CN\cdots H^+\cdots NCCD_3$

Collision energy (eV)	$k(CH_3CNH^+)/k(CD_3CNH^+)$[a]
5	1.16 ± 0.05
10	1.19 ± 0.03
20	1.18 ± 0.01
50	1.18 ± 0.02

[a]Values given as apparent proton affinity ± standard deviation.

dimer will increase. At higher internal energy, entropic effects become increasingly important relative to internal energy effects on the relative rates for the competing dissociation channels. Several previous studies [28,29], as well as the data on the acetonitrile/higher nitrile dimers, demonstrate these points. However, in this case, the observed ratio of rate constants measured as the ratio of product ion abundances for the two pathways, $k(CH_3CNH^+)/k(CD_3CNH^+)$, remains constant, as the collision energy is progressively increased from 5 to 50 eV (Table 4). This suggests that the ions sampled already have considerable precollision internal energy and that the (small) entropic differences between the two dissociation channels for $CH_3CN\cdots H^+\cdots NCCD_3$ control the branching ratio.

The difference in the PA of the two ligands can be estimated for each collision energy from the direct comparison data using the standard kinetic method equation

$$\Delta PA = RT_{eff}\ \ln(k_1/k_2), \tag{10}$$

where T_{eff} is the average temperature obtained from the extended kinetic method analysis for the determination of the PA of the respective acetonitrile. As given in Table 5, the direct comparison of the two acetonitriles reveals that the difference in PA is much smaller than the difference estimated by the extended kinetic method, although it is still within its allowed range. On the basis of the branching ratio of the dissociation of the proton-bound dimer of acetonitrile and d_3-acetonitrile, the PA difference is estimated to be 0.2 kcal mol^{-1}. This value is in reasonable agreement with the value at one collision energy reported by Eberlin et al. [19] of ≈0.3 kcal mol^{-1}.

Table 5
Proton affinity (PA) difference calculated from the dissociation of the proton-bound cluster ions composed of the specified ligands

	ΔPA (kcal mol^{-1})[a]	ΔPA (kcal mol^{-1})[b]
CH_3CN/CD_3CN		
5	0.14	0.83
10	0.19	1.07
20	0.23	1.28
50	0.29	1.63
CH_3CN/C_2H_5CN		
5	2.22	1.72
10	2.36	1.72
20	2.39	1.63
50	2.36	1.39
CD_3CN/C_2H_5CN		
5	2.36	3.99
10	2.48	4.56
20	2.39	4.87
50	2.26	5.42

[a]Proton affinity difference calculated using the standard kinetic method equation (Eq [10]).

[b]Proton affinity difference calculated using the extended kinetic method (Eq. [11]). The entropy difference used for this calculation was obtained from the two relative entropies of protonation for CH_3CN and CD_3CN.

This simple treatment obviously neglects entropy effects when calculating the PA difference. The PA difference between the isotopomers can be estimated by manipulating Eq. (5) to obtain Eq. (11):

$$\Delta PA_{d_3-d_0} = RT_{eff}[\ln(k_1/k_2) + \Delta(\Delta S)_{d_3-d_0}/R]. \tag{11}$$

The experimental branching ratio is that for the dissociation of the proton-bound dimer composed of the two acetonitriles. The term $\Delta(\Delta S_{d_3-d_0})$ corresponds to the difference in protonation entropies of the labeled and nonlabeled compounds. The value of this term is approximated as the difference in entropies of protonation of each isotopomer relative to the alkyl nitriles as obtained by the extended kinetic method. Using this value for $\Delta(\Delta S)_{d_3-d_0}$, and the branching ratio measured for the isotopically mixed dimer, the proton affinity difference between CH_3CN and CD_3CN is found to be ≈1.2 kcal mol^{-1}.

The differences in PA between propionitrile and the two forms of acetonitrile were also investigated

(Table 5). Applying the standard kinetic method, the PA difference between CH_3CN and C_2H_5CN increases gradually from 5 to 20 eV collision energy. A similar trend was observed for the PA difference between CD_3CN and C_2H_5CN. The magnitude of PA difference between CH_3CN/C_2H_5CN (average 2.3 kcal mol^{-1}) is almost identical to that for CD_3CN/C_2H_5CN (average 2.4 kcal mol^{-1}). At higher collision energies there is a crossover, and the difference in PA for CD_3CN/C_2H_5CN becomes smaller. This crossover is the result of excluding entropy effects in the analysis, which is clearly demonstrated when the extended kinetic method (Eq. [11]) is applied to these two systems. For the CH_3CN/C_2H_5CN pair, the PA difference tends to decrease as collision energy is increased (average 1.6 kcal mol^{-1}) from 5 to 50 eV, whereas the CD_3CN/C_2H_5CN pair, the PA difference tends to increase (average 4.7 kcal mol^{-1}). These observations indicate that there is a real difference in PA between CH_3CN and CD_3CN because of isotopic effects. The exact value is difficult to estimate, but the 0.2 kcal mol^{-1} value from the low–collision energy data of the standard kinetic method using the direct comparison is probably more accurate than the value obtained using the extended kinetic method.

4. Conclusions

This investigation explores the use of the standard and extended versions of the kinetic method to provide accurate thermochemical quantities. The ratios of product ions from the dissociation of proton-bound dimers activated at several collision energies are used to estimate the proton affinity of CD_3CN. The method of data analysis detailed by Armentrout [1] is employed, and comparisons to previous methods of data analysis are discussed. The experimental data is also employed in studying the quality of thermochemical information that may be obtained from the standard kinetic method, the Fenselau/Wesdemiotis method of analysis, and the Armentrout data treatment. The different versions of the kinetic method are used to arrive at values for ΔPA and $\Delta(\Delta S)$ for the $CH_3CN\cdots H^+\cdots NCCD_3$ dimer, thus verifying that this method can be used to study small differences in PA between isotopomers.

The PA of d_3-acetonitrile and the relative protonation entropy with respect to the reference compounds used were found to be 186.3 $\pm$ 1.2 ($\pm$1.4) kcal mol^{-1} and 1.8 $\pm$ 0.3 ($\pm$0.3) kcal mol^{-1}, respectively. The values are in good agreement with those obtained using the extended kinetic method of Fenselau and Wesdemiotis: 186.3 $\pm$ 0.2 ($\pm$0.2) kcal mol^{-1} and 1.8 $\pm$ 0.3 ($\pm$0.3) cal mol^{-1} K^{-1}, respectively. However, the errors associated with the former method of analysis are more representative of the true errors of the experiment, in that the second plot of the extended kinetic method is not constructed from quantities that are dependent on each other. The PA of acetonitrile is also determined using the Armentrout analysis (188.2 $\pm$ 1.2 [$\pm$1.4] kcal mol^{-1}) and found to be similar to the PA of d_3-acetonitrile.

The differences in entropies of protonation measured in this study are subject to large errors, but the existence of a real isotope effect is indicated by the change in sign between the d_0/C_n and d_3/C_n series. The entropy of protonation is assumed to be independent of temperature over the range of temperature studied here. However, there are some effects in the experimental data, summarized in the next paragraph, that are not explained and that may compromise the relative entropy measurements.

The kinetic method is also used to investigate kinetic isotope effects deuterium substitution in the dissociation of proton-bound dimers. For the dissociation of the proton-bound dimer composed of acetonitrile and d_3-acetonitrile, a normal secondary kinetic isotope effect is observed. This is consistent with the kinetic method results that show that $PA(CH_3CN) > PA(CD_3CN)$. A direct comparison of the two acetonitriles demonstrates that the PA difference is much smaller than the value obtained (indirectly) using the extended kinetic method. The abundance ratio of the two adducts, CH_3CNH^+ and CD_3CNH^+, (k_H/k_D), remains almost constant, ranging from 1.16 to 1.19 as the collision energy is increased from 5 to 50 eV. On the basis of the branching ratio for the dissociation of the $CH_3CN\cdots H^+\cdots NCCD_3$ dimer, the PA difference is estimated to be $\approx$0.2 kcal mol^{-1}. That the

difference in PA between CD_3CN and CH_3CN obtained using the kinetic method is a true difference and not the result of a statistical error is corroborated by comparing the difference in PA in the CH_3CN/C_2H_5CN dimer to the difference in proton affinity in the CD_3CN/C_2H_5CN dimer. The PA difference in the CH_3CN/C_2H_5CN dimer tends to decrease with increasing collision energy, whereas the ΔPA for the CD_3CN/C_2H_5CN dimer tends to increase. The behavior of the branching ratio of the proton-bound cluster ion composed of the isotopomers of acetonitrile is not fully understood. More typical behavior, observed for the dissociation of each of the acetonitrile isotopomers with the series of alkyl nitrile reference compounds, is a tendency toward unity with increasing energy. These results together with the earlier data of Normann and McMahon indicate that contributions from other isomeric forms of the ions studied cannot be excluded.

Acknowledgements

This work was supported by the Division of Chemical Sciences, Office of Basic Energy Sciences, Office of Energy Research, U.S. Department of Energy (DE-FG02-94ER14470).

References

[1] P.B. Armentrout, J. Am. Soc. Mass Spectrom. 11 (2000) 371.
[2] R.G. Cooks, T.L. Kruger, J. Am. Chem. Soc. 99 (1977) 1279.
[3] S.A. McLuckey, D. Cameron, R.G. Cooks, J. Am. Chem. Soc. 103 (1981) 1313.
[4] R.G. Cooks, J.S. Patrick, T. Kotiaho, S.A. McLuckey, Mass Spectrom. Rev. 13 (1994) 287.
[5] R.G. Cooks, J.T. Koskinen, P.D. Thomas, J. Mass Spectrom. 34 (1999) 85.
[6] S.S. Yang, P. Wong, S.G. Ma, R.G. Cooks, J. Am. Soc. Mass Spectrom. 7 (1996) 198.
[7] W.A. Tao, D.X. Zhang, F. Wang, P.D. Thomas, R.G. Cooks, Anal. Chem. 71 (1999) 4427.
[8] S.L. Craig, M.L. Zhong, B. Choo, and J.I. Brauman, J. Phys. Chem. A 101 (1997) 19.
[9] G. Bojesen, T. Breindahl, J. Chem. Soc. Perkin Trans. 2 (1994) 1029.
[10] X.H. Cheng, Z.C. Wu, C. Fenselau, J. Am. Chem. Soc. 115 (1993) 4844.
[11] B.A. Cerda, C. Wesdemiotis, J. Am. Chem. Soc. 118 (1996) 11884.
[12] M.J. Nold, B.A. Cerda, C. Wesdemiotis, J. Am. Soc. Mass Spectrom. 10 (1999) 1.
[13] P.J. Robinson, K.A. Holbrook Unimolecular Reaction, Wiley-Interscience, London 1972.
[14] J. Laskin, J. Futrell, Journal of Physical Chemistry A 104 (2000) 8829.
[15] L. Drahos, K. Vekey, J. Mass Spectrom. 34 (1999) 79.
[16] P.D. Schnier, J.C. Jurchen, E.R. Williams, J. Phys. Chem. 103 (1999) 737.
[17] J.W. Denault, Ph.D. thesis, Purdue University, December 2000.
[18] K. Normann, T.B. McMahon, Int. J. Mass Spectrom. 182/183 (1999) 381.
[19] F.C. Gozzo, M.N. Eberlin, J. Mass Spectrom. In press 2001.
[20] B.D. Nourse, R.G. Cooks, Int. J. Mass Spectrom. Ion Processes 106 (1991) 249.
[21] T.T. Dang, E.L. Motell, M.J. Travers, E.P. Clifford, G.B. Ellison, C.H. DePuy, V.B. Bierbaum, Int. J. Mass Spectrom. Ion Processes 123 (1993) 171.
[22] R.A. J. O'Hair, S. Gronert, T.D. Williams, Org. Mass Spectrom. 29 (1994) 151.
[23] J.L. Holmes, Org. Mass Spectrom. 20 (1985) 169.
[24] R.G. Cooks, A.L. Rockwood, Rapid Commun. Mass Spectrom. 5 (1991) 93.
[25] J.W. Denault, F. Wang, R.G. Cooks, F.C. Gozzo, M.N. Eberlin, J. Phys. Chem. A 104 (2000) 11290.
[26] K. Norrman, T.B. McMahon, Int. J. Mass Spectrom. 182/183 (1999) 381.
[27] S.G. Lias, J.E. Bartmess, J.F. Liebman, J.L. Holmes, R.D. Levin, and W.G. Mallard, in NIST Chemistry WebBook, W.G. Mallard, P.J. Linstrom (Eds.) National Institute of Standards and Technology, Gaithersburg MD (http://webbook.nist.gov.), 2000; NIST Standard Reference Database Number 69.
[28] S.A. McLuckey, R.G. Cooks, J.E. Fulford, Int. J. Mass Spectrom. Ion Phys. 52 (1983) 165.
[29] G. Chen, R.G. Cooks, D.M. Bunk, M.J. Welch, J.R. Christie, Int. J. Mass Spectrom. 185 (1999) 75.